Fracture Mechanics of Concrete Structures,
Proceedings FRAMCOS-2, edited by Folker H. Wittmann,
AEDIFICATIO Publishers, D-79104 Freiburg (1995)

FRACTURE PARAMETERS FOR CONCRETE BASED ON POLY-LINEAR APPROXIMATION ANALYSIS OF TENSION SOFTENING DIAGRAM

Y. Kitsutaka
Department of Architecture, Tokyo Metropolitan University
Tokyo, Japan

Abstract

Poly-linear approximation analysis method for tension softening diagram (TSD) was proposed based on the cohesive force model (CFM) concept and nonlinear crack equation analysis. Elasto-plastic fracture parameters for concretes such as energy release rate for plastic materials G_p, R-curve, fracture energy, toughness modulus (T.M.), etc. were analyzed based on the energy consumed in cohesive zone calculated by analyzed TSD. Fracture parameters for various concretes were discussed.

1 Introduction

It is pointed out by many researchers that the tension softening diagram (TSD) is a very useful basic parameter characterizing fracture behavior of non-elastic material such as concrete. TSD also could estimate the energy changes in fracture process zone(FPZ), and it gives us a lot of informations on the elasto-plastic fracture parameters, which had been the most important subject in the field of fracture mechanics.

This study aims to propose, 1) new method to determine the complete TSD from a load-displacement curve, 2) the elasto-plastic fracture parameter based on TSD analysis, 3) toughness parameter which can estimate the very ductile materials such as FRC or Hyper-concrete.

2 Poly-linear approximation analysis of tension softening diagram

2.1 Cohesive force model analysis with poly-linear TSD

In this study, TSD was analyzed by using the cohesive force model(CFM) analysis method as shown in Fig.1. The dugdale-barenblatt type TSD can be expressed by poly-linear curve as shown in Fig. 2. The cohesive stress $\sigma(x, a)$ is the poly-linear function of crack opening displacement(COD) δ

$$\sigma(a,x) = m(\delta)\cdot\delta + n(\delta), \quad \delta = \delta(a,x) \tag{1}$$

where, a is the crack length, x is the point on crack surface, $m(\delta)$ is defined as the softening inclination, $n(\delta)$ is the inflection point which is the function of initial σ_0 and $m(\delta)$. So the TSD prediction problem is summarized to obtain appropriate σ_0 and $m(\delta)$.

The boundary conditions of the cracked specimen with cohesive forces are provided by the equilibrium of stress intensity factor in Eq.(2) and the equilibrium of COD in Eq.(3).

$$K(a) = K_p(a) + K_r(a) = 0 \tag{2}$$
$$\delta(a,x) = \delta_p(a,x) + \delta_r(a,x) \tag{3}$$

where, $K(a)$, $K_p(a)$, $K_r(a)$ are the stress intensity factor on crack tip, due to the total force, the external load and the cohesive stress, and $\delta_p(a, x)$,$\delta_r(a, x)$ are the COD due to the external load and the cohesive stress.

These relationship can be solved by using FEM or BEM, but simple beam case, the solution can be obtained by using the calculation results of linear fracture mechanics. For the calculation of COD, Castigliano's theorem was applied (Tada 1975). Then the simple crack integral equation is obtained as Eq.(4). $H(a, x, c)$ is the weight function.

$$\delta(a,x) = \int_0^a \sigma(a,c)\cdot H(a,x,c)dc \tag{4}$$

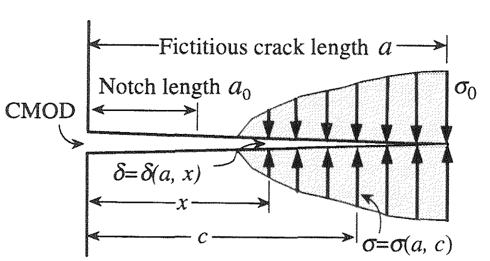

Fig. 1. Cohesive force model(CFM)

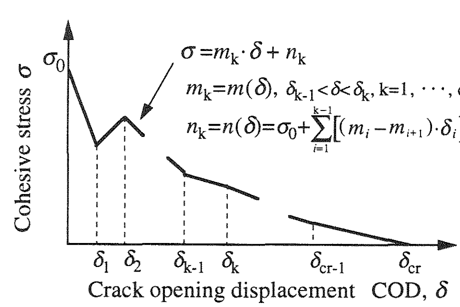

Fig. 2. Poly-linear TSD

From the Eq.(4) and a constitutive law of Eq.(1), the simultaneous equation, called crack equation, is obtained. In poly-linear TSD case, the coefficient of $m(\delta)=m_k$ is the function of the δ as the solution of this equation. This problem can be solved by performing several iterations by changing the appropriate k of m_k in each node after the calculation (Kitsutaka et al. 1994). The relationship of external load and load point displacement (L-LPD) curve is calculated based on the COD distribution and a weight function.

2.2 Back analysis method of poly-linear TSD

Kitsutaka et al. (1994) showed the concept of analyzing the poly-linear TSD by a L-LPD curve. Fig.3 shows the relation of crack propagation and analyzed TSD as the concept of the analysis. The softening inclination m_k and COD of node-1 at step-k (δ_{k1}) were determined by minimizing between the load calculated by a crack equation analysis and the load obtained by an experiment. In this step, former values of all m_k and δ_{k1} were fixed and they were used as constitutive law for calculation. This method can be summarized as that, the relation of COD and cohesive stress on node-1 is calculated with considering the boundary conditions of all nodes for each steps. Because of the monotonous increasing of COD from a crack tip to a crack mouth, in the case of uniform materials, the COD of the node-1 is the largest in anytime, therefore the constitutive law for all COD should be existed for each steps and optimum TSD should be obtained.

The Young's modulus E and σ_0 can be determined by analyzing the initial inclination of L-LPD curve. Between this initial analysis, the softening inclination was temporary assumed to be the constant value.

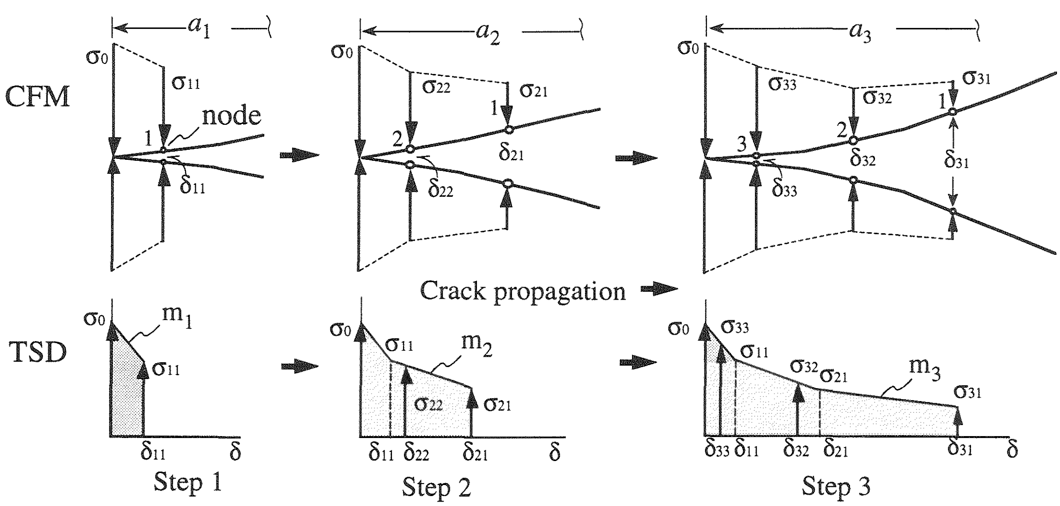

Fig. 3. Concept of poly-linear approximation analysis of TSD

3 Elasto-plastic fracture parameters based on TSD

3.1 Energy release rate of cohesive force model (CFM)

The energy consumed by fracturing can be calculated by considering the energy changes of FCM. Total work done by cohesive forces (dW_f) while the crack propagated da is given as Eq.(5) (see Fig.4).

$$dW_f = t \cdot \int_{a_0}^{a} \left[\sigma(\delta) \cdot \Delta\delta\right] dx \tag{5}$$

where, t is the thickness of specimen. We define the G_p as the energy release rate of CFM, which is obtained by dividing the dW_f by crack propagating area (defined by $dA=t \cdot da$) as Eq.(6). In this study, the fictitious crack advance is included in the general crack propagation. G_p is also, the elasto-plastic fracture parameter, the crack resistance R, and the relation of a and R is the R-curve of CFM.

$$G_p = R = \frac{\partial W_f}{\partial A} = \int_{a_0}^{a} \sigma(\delta) \frac{\partial \delta}{\partial a} dx \tag{6}$$

On the other hand, Energy changes is calculate by the J-integral of CFM showed as famous Eq.(7). But according to the right side of Eq.(7), the energy change is independent to the distribution of COD and only depends on TSD and the value of CTOD. This is because the J-integral of Eq.(7) as the energy release rate is assuming $\partial\delta / \partial a = -\partial\delta / \partial x$ and this indicates that the crack propagation should be the parallel motion. However, in case of concrete, which has large sized process zone, tends to show the COD distribution changing with the crack propagation. So Eq.(6) is more accurate to estimate the energy changes in FPZ.

$$J = -\frac{\partial \Pi}{\partial a} = -\int_{\Gamma} T \frac{\partial u}{\partial x} ds = -\int_{a_0}^{a} \sigma(\delta) \frac{\partial \delta}{\partial x} dx = \int_{0}^{CTOD} \sigma(\delta) d\delta \tag{7}$$

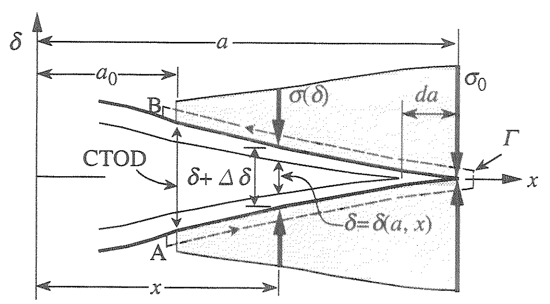

a) Fictitious crack advance

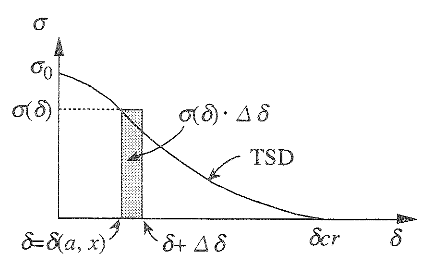

b) Energy consumption at point x

Fig. 4. Fictitious crack advance and energy consumption

The unit energy which is consumed by dividing the fictitious crack surface completely ($\delta = \delta_{cr}$) is same as the area surrounded by TSD under the assumption that the TSD, material property, is same at all ligament. This value is so called fracture energy and expressed as

$$G_F^{TSD} = \int_0^{\delta_{cr}} \sigma(\delta) d\delta \tag{8}$$

and differs from the crack propagating energy G_p as we defined.

3.2 Prediction of energy changes by fracturing

Fig. 5 shows the energy consumption in L-LPD curve. In this figure, unloading curve is approximated for linear line. The relation of energy consumed by fracturing dU_f, the external work dU_w, elastic strain energy dU_e, is

$$dU_f = dU_w - dU_e \tag{9}$$

U_w is measured by L-LPD curve obtained from the result of fracture toughness test as shown in Fig. 5-b).

$$U_w = \mathrm{OBHO} = \int_0^u P du \tag{10}$$

We assume that the energy calculated from G_p as Eq(6). is effectively consumed for the fracturing, so U_f is

$$U_f = \mathrm{OBCO} = t \cdot \int_{a_0}^{a} G_p \, da \tag{11}$$

Elastic strain energy U_e is calculated as shown in Fig. 5-b).

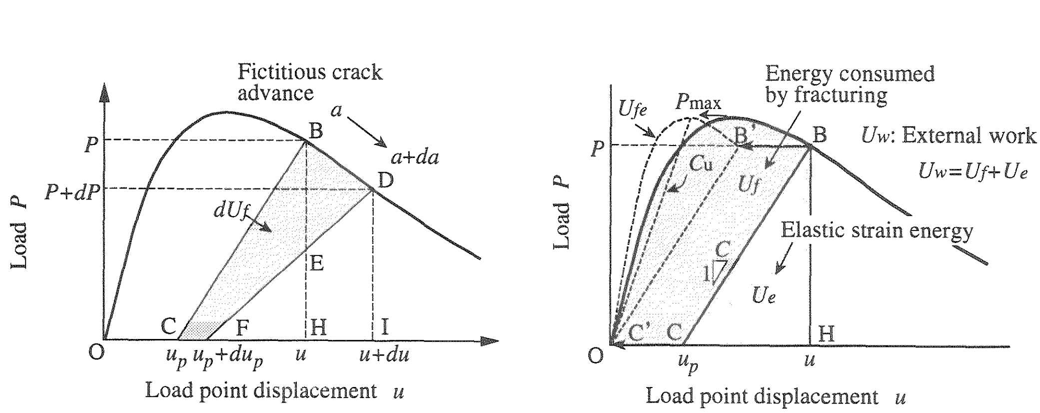

a) Consumed energy dU_f b) Energy dU_f

Fig. 5. Relation of L-LPD curve and energy consumption

$$U_e = \mathrm{OBHO} - \mathrm{OBCO} = U_w - U_f \tag{12}$$

From the U_e, a compliance of any points on L-LPD curve is obtained as

$$C_u = \frac{2 \cdot U_e}{P^2} \tag{13}$$

and from the C_u, we can predict the unloading line. Also we can evaluate the two-parameter K_{Ic}^s and $CTOD_C$, proposed by Jenq and Shah (1985), by calculating C_u at maximum load P as shown in Fig. 5-b) without performing an off-set test but only measuring a L-LPD curve.

Finally many fracture parameters are estimated from the crack analysis of CFM with using TSD analyzed by poly-liner approximation analysis. This procedure is showed in Fig. 6 and Fig. 7.

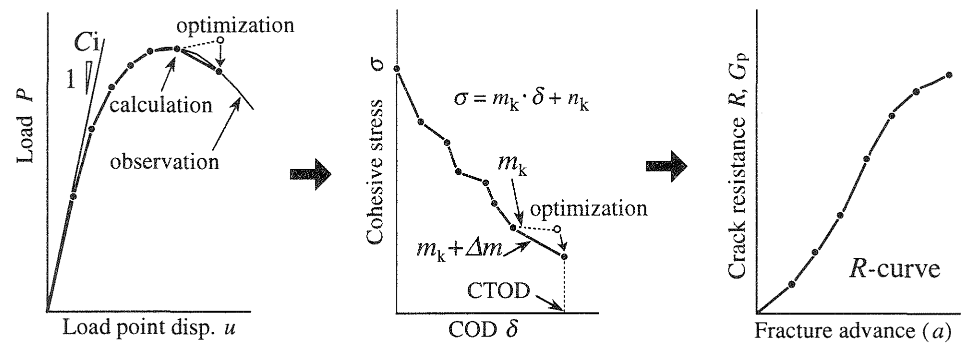

Fig. 6. Procedure of fracture parameter analysis

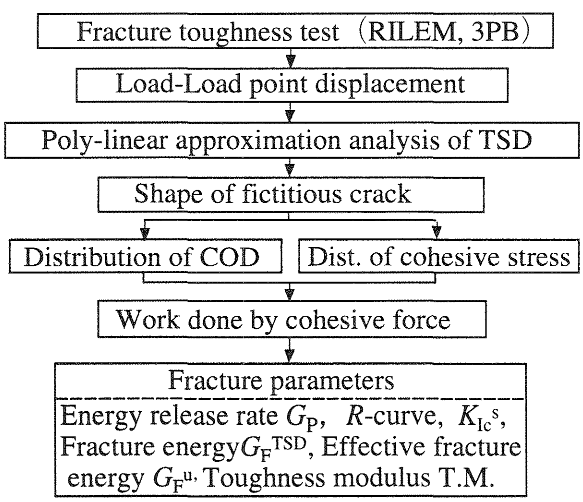

Fig. 7. Analysis flow of fracture parameters

4 Comparison of off-set test results and analysis result

4.1 Outline of off-set test

Two different types of mix proportions were arranged to produce the normal strength concrete specimen (NSC) and the high strength concrete specimen (HSC). The type of aggregate is Gravel of 20mm maximum size. Table 1 shows the mix proportions and properties of concrete. Super plasticizer (SP) and silica fume (SF) were used for HSC.

Three-point bending tests for center notched beam specimen were conducted to measure the L-LPD curves. Specimen size, span length, notch length were 100 x 100 x 450mm, 400mm, 50mm. Specimen was loaded and unloaded. Load was measured by a load cell with 5N sensitivity, and LPD was measured by using two LVDT with 0.001mm sensitivity. LVDT were attached on a support hanging on a specimen to avoid the displacement measurement error caused by load point caving.

Table 1. Mix proportions and fracture parameters of concrete

Sign	W/B	Unit weight (kg/m³)						fc	ft	E	P_{max}	u_0	G_F^{WOF}	E_{cal}	σ_0	δ_{cr}	G_F^{TSD}	K_{Ic}^{S}	CTODc
	%	W	C	SF	S	G	SP	MPa	MPa	GPa	N	mm	N/m	GPa	MPa	mm	N/m	MPa $\cdot m^{1/2}$	mm
NSC	50	184	367	0	777	1064	0	45.3	3.9	31.7	2.40	0.920	120	29.1	6.1	0.197	115	1.05	0.0068
HSC	15	112	673	168	466	1064	29	99.7	5.7	38.6	3.49	0.825	132	42.1	10.7	0.283	123	1.43	0.0067

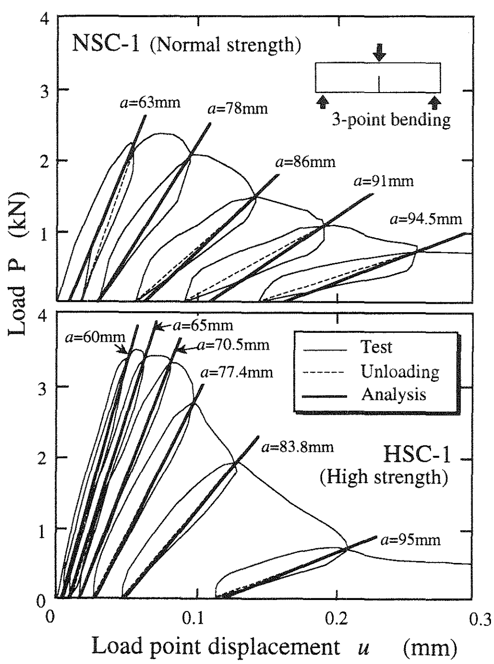

Fig. 8. Off-set test results

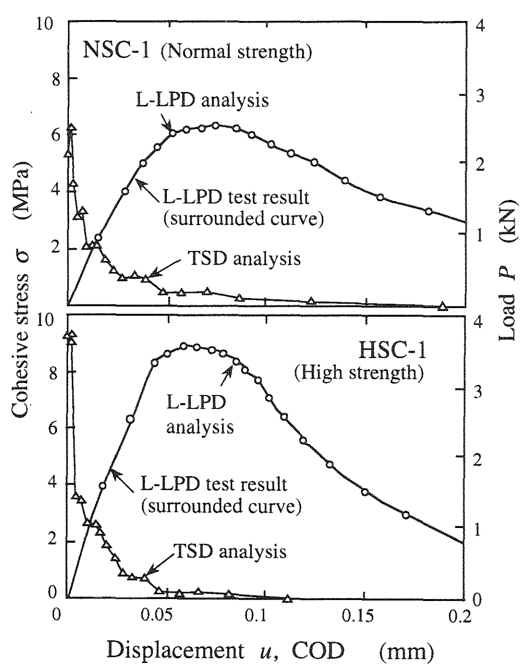

Fig. 9. L-LPD curve and TSD

4.2 Results and discussions

Fig. 8 shows the typical L-LPD curves of off-set tests. The surrounded curve of off-set L-LPD curve is traced in Fig. 9. In this figure, TSD which has been calculated from the traced L-LPD curve by the present analysis method is also showed. The points indicated on L-LPD curves are the calculated values which has been analyzed by the crack analysis method mentioned section 2 with using the calculated poly-linear TSD as a constitutive equation. The observed L-LPD curve and the calculated points are agreed well, so this back analysis method is considered to be an appropriate method to calculate TSD.

In Fig. 8, unloading lines which have been calculated by the analyzed G_p is showed with respect to the approximated unloading line of measured off-set test results. There are agreed well and this means that the energy consumption by fracturing can be predicted by G_p. The optimum fictitious crack lengths a which are calculated in the analysis procedure are also indicated in Fig. 8. The other fracture parameters analyzed by TSD and G_p are summarized in Table. 1.

R-curve of cohesive force model (CFM) is showed in Fig. 10. In case which small fictitious crack length a, G_p and the J-integral of CFM are almost same, but with the increase of a , J-integral are reached to the constant value of $G_F{}^{TSD}$ as indicated in Eq.(7), and this tendency is different from G_p because of J-integral neglecting the fictitious crack figure changes.

It is noted that, G_p of HSC is higher than that of NSC at the small a area, but the area a>90mm, NSC is higher than HSC. This means that the fracture process zone of NSC become larger than HSC with the increase of failure. This is because the failure mode of NSC is the aggregate interfacial cracking and not the transgranular cracking observed in HSC.

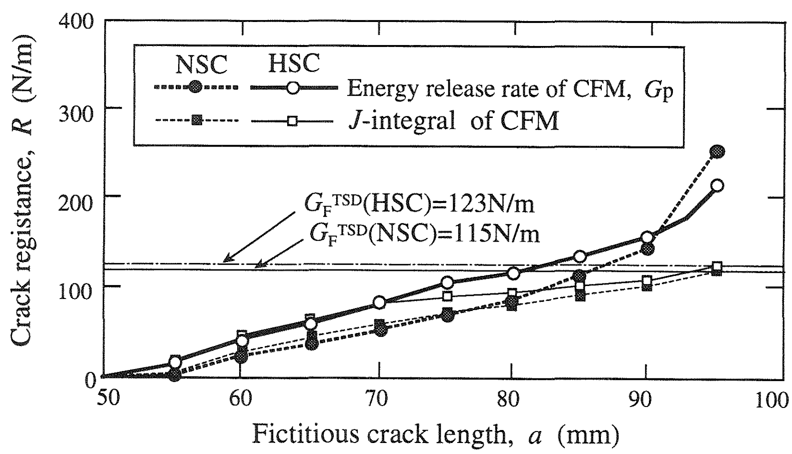

Fig. 10. R-curve of cohesive force model (CFM)

4 Toughness parameters of Hyper-concrete

High-strength, high-toughness concrete will be needed to manufacturing the high-rise RC building which will be safe against the earthquake, etc. We call this type concrete as "Hyper-concrete" and the effective method to producing it is mixing the fiber in HSC. We need the estimation method for the ductility of Hyper-concrete based of fracture mechanics.

G_F and TSD can be the parameter for ductility estimation, however, in case of FRC the critical COD of TSD is very large and toughness depends on the shape of TSD. Fig.11 shows the concept of toughness parameters obtaining from poly-linear TSD. Toughness modulus (T.M.), which is considering the influence of TSD shape on the toughness, is defined by summarizing the local fracture energy g_i as shown in Fig. 11 on the basis of highly estimating the energy absorption in small COD area. $G_F{}^u$ is the effective fracture energy for estimating the very ductile material. The critical COD limitation (δ_u) is set to 0.5mm as the viewpoint of safety of concrete durability. Fig.12-b) shows the L-LPD curves which were calculated based on the various shaped TSD as shown in Fig.12-a). T.M. is a proper parameter, because L-LPD curve becomes ductile with the increase of T.M. regardless of same G_F of 100N/m.

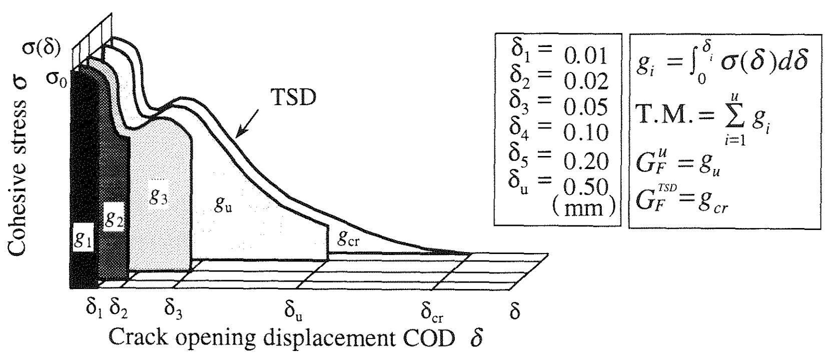

Fig. 11. Fracture toughness parameters based on poly-linear TSD

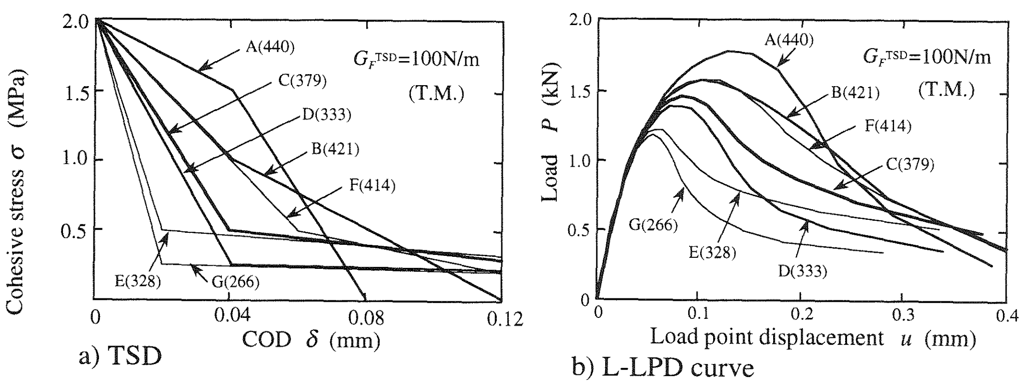

Fig. 12. Relation of T.M. and L-LPD curve with same fracture energy of TSI

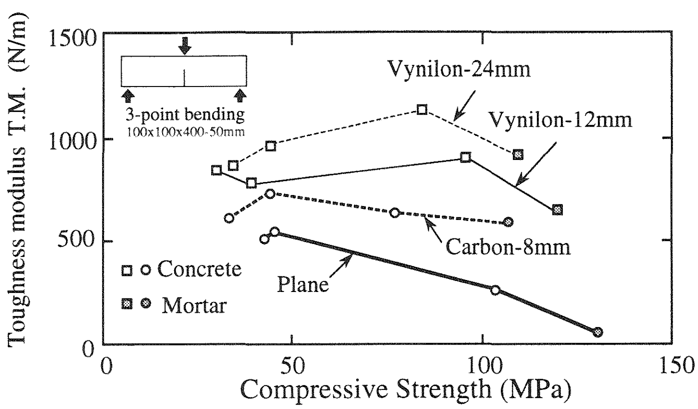

Fig. 13. Toughness modulus(T.M.) and compressive Strength

Fig. 13 shows the relation of T.M. and compressive strength for the various fiber reinforced concretes. Specimen conditions are sowed in figure. In case of plane specimen, with the increase of compressive strength, T.M. becomes low and showed brittle state. In case of the fiber specimen, especially Vinylon-24mm type, T.M. becomes higher than that of plane specimen. This indicates the provability of producing Hyper-concrete. But in case of w/c=15% level, we could not mixed fiber because of consistency problem, so the development of high performance fiber and admixture will be the important future work.

5 Conclusions

1) A new method to determine the tension softening diagram of concrete was proposed based on the poly-linear approximation analysis.
2) Elasto-plastic fracture parameters of concrete were proposed based on the cohesive force model concept and the analysis of poly-linear tension softening diagram.
3) Toughness parameters for fiber concretes (normal strength, high-strength, hyper) was proposed.

References

Jenq, Y.S. and Shah, S.P. (1985), Two parameter fracture model for concrete. **J. of Engrg.Mech., ASCE**, 111, (10), 1227-1241.

Kitsutaka, Y., Kamimura, K., and Nakamura, S. (1994) Evaluation of aggregate properties on tension softening behaviour of high strength concrete, **High Performance Concrete** ACI SP149-40, 711-727.

Tada, H., Paris, P.C. and Irwin, G.R. (1985), **The stress analysis of cracks handbook**. Paris Productions Incorporated, 2-16, 27.